Food Microbiology 84 (2019) 103267

Contents lists available at ScienceDirect

Food Microbiology

journal homepage: www.elsevier.com/locate/fm

Effect of microstructure and initial cell conditions on thermal inactivation kinetics and sublethal injury of *Listeria monocytogenes* in fish-based food model systems

Davy Verheyen[a,b,c,1], Maria Baka[a,b,c,1], Simen Akkermans[a,b,c,1], Torstein Skåra[d], Jan F. Van Impe[a,b,c,*,1]

[a] BioTeC+ - Chemical and Biochemical Process Technology and Control, KU Leuven, Gebroeders de Smetstraat 1, 9000, Gent, Belgium
[b] OPTEC, Optimization in Engineering Center-of-Excellence, KU Leuven, Belgium
[c] CPMF^2, Flemish Cluster Predictive Microbiology in Foods, Belgium
[d] Nofima, P.O. Box 8034, 4068, Stavanger, Norway

ARTICLE INFO

Keywords:
Food safety
Predictive microbiology
Thermal inactivation
Sublethal injury

ABSTRACT

The development of more accurate predictive models that describe the microbial kinetics of mild thermal treatments of foods requires knowledge concerning the influence of food microstructure and initial cell conditions on foodborne pathogens' inactivation kinetics. The effect of food microstructure and initial cell conditions on thermal inactivation kinetics and sublethal injury (SI) of *Listeria monocytogenes* was investigated at 59, 64 and 69°C. Fish-based food model systems with different microstructures, possessing minimal compositional and physicochemical variations, were used. *L. monocytogenes* growth morphology had no significant influence on thermal inactivation kinetics. A gelled matrix resulted in a lower specific inactivation rate k_{max} and a higher residual cell population N_{res}, while the presence of fat droplets resulted in a higher k_{max} and did not influence N_{res}. SI was higher in viscous than in gelled systems and more prominent for cells that were grown inside the matrix. Hence, predictive thermal inactivation models could benefit from the inclusion of factors related to the nature of the food matrix and fat properties. Starting inactivation from cells that were grown inside the matrix, resulted in lower (i.e., fail-safe) k_{max} values and more uncertainty on N_{res} as compared to starting from cells grown at optimal conditions.

1. Introduction

The bacterium *Listeria monocytogenes*, causing listeriosis, is one of the most heat tolerant non-spore forming food pathogens (Farber and Peterkin, 1991). Therefore, ready-to-eat food products which are subjected to a mild heat treatment are very susceptible to *L. monocytogenes* contamination (Ates et al., 2014), and fish products especially (Ben Embarek, 1994). *L. monocytogenes* was detected in 4.7% of sampled fish products across all sampling stages (i.e., processing and retail) in Europe in 2016 (EFSA European Food Safety Authority, ECDC European Centre for Disease Prevention and Control, 2017). Due to its high resistance to various stresses, *L. monocytogenes* is also very relevant for the validation of microbial inactivation processes of other non-sporulating bacteria (Baka et al., 2015).

In food industry, thermal processing remains one of the most important methods of reducing/avoiding the presence of foodborne pathogens such as *L. monocytogenes* in food products (Álvarez-Ordóñez et al., 2008; Rawson et al., 2011; Wang et al., 2017). In recent decades, a trend towards milder thermal treatments is observed due to the increasing consumer demand for high-quality and safe foods (Devlieghere et al., 2004; Rajkovic et al., 2010; Smelt and Brul, 2014). Specifically, for fish products, rapid or minimal heating processes that ensure the required safety level are beneficial, since those products are particularly susceptible to consequences of excessive thermal treatments (*e.g.*, dry structure, flaking) (Rosnes et al., 2011; Skåra et al., 2002; Skipnes et al., 2008). For the case of *L. monocytogenes*, a temperature of 70 °C (inner part of the product) for 2 min is required to achieve a 6-log reduction of cells, although equivalent inactivation can be achieved at temperatures

* Corresponding author. Chemical and Biochemical Process Technology and Control (BioTeC+) Department of Chemical Engineering, KU Leuven, Gebroeders de Smetstraat 1, B-9000, Gent, Belgium.
E-mail addresses: davy.verheyen@kuleuven.be (D. Verheyen), maria.baka@kuleuven.be (M. Baka), simen.akkermans@kuleuven.be (S. Akkermans), torstein.skara@nofima.no (T. Skåra), jan.vanimpe@kuleuven.be (J.F. Van Impe).
[1] www.cpmf2.be.

https://doi.org/10.1016/j.fm.2019.103267
Received 26 July 2018; Received in revised form 22 May 2019; Accepted 10 July 2019
Available online 11 July 2019
0740-0020/

as low as 60 °C (treatment time of approximately 45 min) (Rosnes et al., 2011). However, a considerable subpopulation of bacteria subjected to mild thermal treatments is not killed but sublethally injured (Besse, 2002). Sublethal injury is defined as "a consequence of exposure to a chemical or physical process that damages but does not kill a microorganism" (Hurst, 1977). The injury can either be structural (i.e., altered membrane permeability) or metabolic (i.e., damage to functional cell components), or a combination of both (Brashears et al., 2001; Wang et al., 2017). Sublethally injured cells are more challenging to detect in food industry (i.e., due to their inability to form visible colonies on selective media) and may recover after thermal treatments, leading to enhanced resistance to various stresses (Jasson et al., 2007; Noriega et al., 2013; Silva et al., 2015; Skandamis et al., 2008; Wu, 2008).

Predictive microbiology is a discipline of food microbiology in which microbial responses in food products are studied under controlled intrinsic (e.g., pH) and extrinsic (e.g., temperature) conditions in order to develop mathematical models for response prediction (McMeekin et al., 2002; Van Impe et al., 2005). Most predictive models are developed based on experiments in liquid model systems, which may have limited predictive value when the models are validated in real food products (Pin et al., 1999). Furthermore, thermal inactivation experiments are traditionally conducted by inoculating the food product or model system (i.e., surface or homogeneous inoculation) with a high number of cells grown at optimal conditions (Gurtler et al., 2011; Khoo et al., 2003; Mastwijk et al., 2017; Reichart, 1994; Wang et al., 2017). In food industry, however, food products contaminated with a small number of cells which can grow in the product prior to thermal inactivation, form a more realistic scenario (Annous et al., 1999; Bellara et al., 2000; Farber and Peterkin, 1991). Since thermal inactivation kinetics of pathogens like *L. monocytogenes* are influenced by the growth conditions prior to the thermal treatment (Aryani et al., 2015; Edelson-Mammel et al., 2005; Schultze et al., 2007), the applicability of predictive models developed based on experiments started from a high number of cells grown at optimal conditions might be limited. Hence, a more detailed knowledge of the influence of food microstructure and initial cell conditions on inactivation kinetics of foodborne pathogens could be used to refine the accuracy of predictive models for the food industry.

Food microstructure relates to the spatial arrangement and interactions of the structural elements of a food product (e.g., droplets, air cells, crystals, strands, micelles and interfaces), as well as the resulting architecture of these combined elements (Aguilera, 2009; Heertje, 1993). Microstructural factors that influence thermal inactivation kinetics include the presence and concentration of fat (Juneja et al., 2001; Oliveira et al., 2018; Passos and Kuaye, 2002; Schultze et al., 2007; Szlachta et al., 2010), the nature of the food matrix (i.e., liquid/viscous, gelled/solid) (Bellara et al., 1999; Mackey et al., 2006; Murphy et al., 2000; Velliou et al., 2013; Wang et al., 2017), rheological properties of the food matrix (Velliou et al., 2013), and bacterial growth morphology (*e.g.*, colony size) (Noriega et al., 2013; Velliou et al., 2013). One method to acquire more fundamental insight into the effect of food microstructure on microbial inactivation kinetics and develop more accurate predictive models, is the use of model systems with various microstructures (Baka et al., 2016, 2017a, 2017b). However, in most thermal inactivation studies which used this method, the observed differences in microbial dynamics were possibly caused (in part) by varying compositional and physicochemical factors among the different model systems, a consequence of developing model systems with varying microstructural complexity (Murphy et al., 2000; Wang et al., 2017). In addition, those studies focussed on the comparison of two microstructures, rather than on the entire microstructural spectrum of food products, introduced by Wilson et al. (2002), i.e., liquids, aqueous gels, oil-in-water emulsions, water-in-oil emulsions, gelled emulsions, and surfaces.

In this study, the isolated influence of food microstructure on inactivation kinetics of *L. monocytogenes* at 59, 64 and 69°C was investigated, using model systems among which the microstructural effect was effectively isolated (Verheyen et al., 2018a). These model systems represented the entire microstructural spectrum present in food products, consisting of three viscous systems (i.e., a liquid, xanthan (a more viscous liquid system), and an emulsion) and two gelled systems (i.e., an aqueous gel and a gelled emulsion). Major food microstructural elements (*e.g.*, fat droplets, a visco-elastic matrix) were present in these model systems, while their composition was based on processed fish products, *e.g.*, fish soup (structure similar to liquid or xanthan system), surimi (aqueous gel), fish salad (emulsion), fish paté (gelled emulsion). This way, the effect on inactivation parameters of bacterial growth morphology (*e.g.*, colonies or single cells, colony sizes), the nature of the food matrix (i.e., viscous vs. gelled), and the presence of fat droplets was studied systematically, an important difference compared to previous studies in the field. Temperature evolution in the model systems was recorded during thermal treatments. By starting thermal inactivation experiments from two different initial cell conditions (i.e., (i) cells grown inside the model system matrix and (ii) cells grown at optimal conditions), it was investigated whether the thermotolerance of *L. monocytogenes* is affected when cells are grown inside the food matrix. For all aforementioned conditions, the influence of microstructural aspects and initial cell conditions on the sublethal injury of *L. monocytogenes* was also investigated.

2. Materials and methods

2.1. Model system preparation

Fish-based model systems with various microstructures were prepared and used as described in Verheyen et al. (2018a), using small vials (4 mL, 45 × 14.7 mm, BGB Analyti Benelux B.V., Harderwijk, the Netherlands) containing 1 mL (i.e., height of approximately 10 mm) of viscous or structured medium. The set of model systems consisted of three viscous (i.e., liquid, xanthan, emulsion) and two gelled systems (i.e., aqueous gel, gelled emulsion), covering the range of microstructures present in common food products in correspondence with the classification of Wilson et al. (2002). The composition, pH and water activity (a_w) of the different model systems is shown in Table 1. Model systems consisted of hydrolysed fish protein (ProGo™, Hofseth Biocare ASA, Ålesund, Norway), sodium alginate (Sigma-Aldrich, MO, USA), NaCl (Sigma-Aldrich, MO, USA), $CaCO_3$ (Sigma-Aldrich, MO, USA), D-(+)-gluconic acid δ-lactone (GDL, Sigma-Aldrich, MO, USA), sunflower oil (Eldorado, local supermarket, Stavanger, Norway), Tween 80 (Sigma-Aldrich, MO, USA), Span 80 (Sigma-Aldrich, MO, USA), Xanthan gum (Sigma-Aldrich, MO, USA), and H_2O. More information regarding the model systems (*e.g.*, detailed preparation protocol, rheological properties, texture, fat droplet size distribution) can be found in the study of Verheyen et al. (2018a).

2.2. Microorganisms and preculture conditions

L. monocytogenes strains LMG 23773, LMG 23774 (both isolated from smoked salmon), and LMG 26484 (isolated from tuna salad), were acquired from the BCCM/LMG bacteria collection of Ghent University in Belgium. Stock cultures were stored at −80 °C in 80% (v/v) Brain Heart Infusion Broth (BHI, VWR International, Leuven, Belgium) and 20% (v/v) glycerol (Acros Organics, Geel, Belgium). For each strain, a purity plate was prepared separately by spreading a loopful of stock culture onto a BHI Agar plate (1.4% (w/v), Agar Technical No3, Oxoid Ltd., Basingstoke, UK), which was subsequently incubated at 30 °C for 24 h. One colony of the purity plate was carefully transferred into 20 mL of BHI. After incubating for 24 h at 30 °C under static conditions, 20 μL of the stationary-phase culture was inoculated into 20 mL of fresh BHI and incubated for 24 h under the same conditions. This resulted in stationary phase *L. monocytogenes* cultures with an inoculum level of

Table 1
Composition, pH and a_w of the different model systems (Verheyen et al., 2018a). Concentration of the components is expressed as % w/w.

	Liquid	Xanthan	Emulsion	Aq. gel	Gelled emulsion
Protein	5.00	5.00	5.00	5.00	5.00
Alginate	3.00	3.00	3.00	3.00	3.00
NaCl	0.96	0.96	0.95	0.95	0.94
$CaCO_3$	/	/	/	0.40	0.40
GDL	/	/	/	0.96	0.95
Sunflower oil	/	/	1.00	/	1.00
Tween 80	/	/	0.10	/	0.10
Span 80	/	/	0.20	/	0.20
Xanthan gum	/	0.50	0.50	/	/
H_2O	91.04	90.54	89.25	89.69	88.41
pH (± SD)	6.36 ± 0.16	6.34 ± 0.01	6.35 ± 0.01	6.43 ± 0.18	6.34 ± 0.11
a_w (± SD)	0.989 ± 0.001	0.987 ± 0.002	0.988 ± 0.001	0.985 ± 0.001	0.985 ± 0.003

approximately 10^9 CFU/mL. From each of the three cultures, 10 mL was pooled in a 100 mL Erlenmeyer under aseptic conditions and mixed, resulting in a *L. monocytogenes* strain cocktail with a cell density of 10^9 CFU/mL (Verheyen et al., 2018b).

2.3. Inoculation conditions

In order to assess the influence of initial cell conditions on thermal inactivation kinetics, experiments were conducted using *L. monocytogenes* cells which were grown to a high cell density level in two different ways: (i) cells grown inside the model system matrix and (ii) cells grown at optimal conditions. A schematic representation of both inoculation methods is provided in Fig. 1. In the case where cells were grown inside the matrix, model systems were inoculated to a cell density of 10^2 CFU/mL using a NaCl solution of 0.90% (w/v) as dilution medium, distributed over the small vials, and incubated at 10 °C for 14 days prior to the inactivation experiment. This resulted in stationary phase cells with a cell density of approximately 10^8–10^9 CFU/mL (Verheyen et al., 2018b). For gelled systems, the inoculation took place prior to the initiation of the gelation reaction, as described in Verheyen et al. (2018a). In the case where cells were grown at optimal conditions, model systems were directly inoculated to a cell density of 10^8–10^9 CFU/mL from a fresh preculture. 30 mL of the strain cocktail was transferred to a falcon tube and centrifuged at 18,500 g for 15 min at 4 °C. Afterwards, the supernatant was carefully removed and the pellet was added to 100 g of the respective model system. The model system was thoroughly mixed and distributed over the small vials, which were stored at 10 °C for approximately 16 h prior to the inactivation experiment. Based on preliminary experiments, this short incubation period was determined to not result in a significant increase in cell levels. Consequently, inactivation experiments were started from model systems with a cell density of 10^8–10^9 CFU/mL for both inoculation conditions. In both cases, inactivation was started from stationary phase cells, since these are more heat resistant than exponentially growing populations (Aryani et al., 2015; Noriega et al., 2013; Smelt and Brul, 2014).

2.4. Thermal inactivation experiments

Thermal inactivation experiments were conducted in a water bath at a constant temperature of 59, 64 or 69°C. The small vials containing the inoculated model systems were placed in a rack which was carefully lowered into the water bath. At different time points, one vial was transferred from the water bath to an ice water bath (i.e., temperature of approximately 0 °C) in order to stop the inactivation, and kept inside for maximum 3 h before further processing steps. For viscous systems

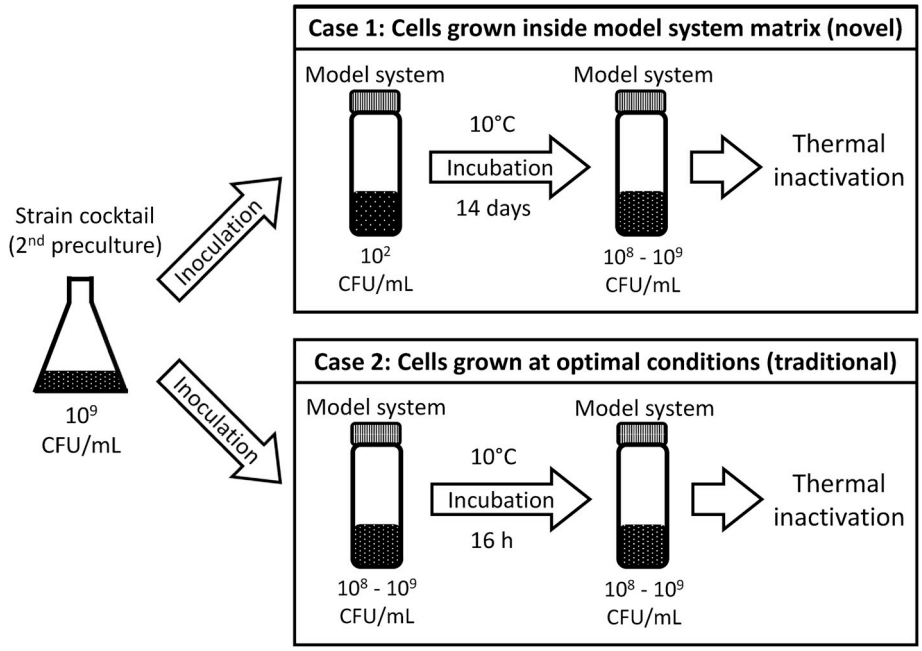

Fig. 1. Schematic overview of the two inoculation conditions which were used for the thermal inactivation experiments: (i) cells grown inside the model system matrix and (ii) cells grown at optimal conditions.

(i.e., liquid, xanthan, and emulsion), serial decimal dilutions were directly prepared from an aliquot of the samples using NaCl solution of 0.90% (w/v) and afterwards plated on BHI and PALCAM agar (PALCAM *Listeria* Selective Agar, according to Van Netten et al. (1989), Merck Millipore, Darmstadt, Germany), employing the drop technique (Herigstad et al., 2001). While drops of 20 µL were plated for dilutions 10^{-1} to 10^{-6}, drops of 100 µL were plated for the undiluted sample in order to acquire a lower detection limit (DL). For gelled systems (i.e., aqueous gel and gelled emulsion), the protocol of Hamoud-Agha et al. (2013) was used. More specifically, gels were removed from the vials and transferred into a sterile stomacher bag under aseptic conditions. Subsequently, the vials were rinsed and drained into the bag with 1.5 mL of Phosphate Buffered Saline (PBS, Sigma Aldrich, MO, USA). Afterwards, 1.5 mL of McIlvaine buffer (0.2 M Na_2HPO_4, Sigma Aldrich, MO, USA; 0.1 M citric acid, Acros Organics, NJ, USA) was added to the bag in order to initiate gel breakdown. The mixture was homogenised for 10 min (basic masticator, Led techno, Heusden-Zolder, Belgium), after which serial decimal dilutions were plated similarly to the viscous systems. Finally, the plates were incubated at 30 °C for approximately 30 h before enumeration. Cell counts were considered significant when more than 9 colonies *per* two drops of 100 µL were counted on the agar plates for the undiluted sample, resulting in a DL of 1.7 log (CFU/mL) for viscous systems and 2.3 log (CFU/mL) for gelled systems. The higher DL for gelled systems was due to the extra dilution step caused by the addition of PBS and McIlvaine buffer to the samples. Every experiment was independently performed in triplicate.

2.5. Temperature measurements

Temperature evolution during thermal treatments was measured using a Testo 176 T4 temperature datalogger connected to two TC Type K temperature probes (Testo SE & Co. KGaA, Lenzkirch, Germany). For each temperature (i.e., 59, 64 and 69°C) and model system (i.e., liquid, xanthan, emulsion, aqueous gel, gelled emulsion), water bath and sample temperature during the thermal inactivation experiments were recorded. Vials with the respective model systems were placed in the water bath together in a rack and the probe was placed inside a vial in the middle of the rack. By placing the probe in such a way that the tip of the probe was located in the centre of the model system, the core-temperature in the model systems was recorded for the period of the respective inactivation experiment. Simultaneously, the temperature of the water inside the water bath was also measured using another probe. The temperature in the model systems and the water bath was recorded every 2 s and all temperature measurements were independently performed in triplicate. Temperature data were acquired using ComSoft Basic 5 logger software (Testo SE & Co. KGaA, Lenzkirch, Germany).

Come-up time (CUT) was defined as the time needed to increase the core temperature of the model systems to a temperature equal to 99% of the maximum (constant) core temperature (Chung et al., 2008). CUT for a single model system at a single temperature was calculated as the average CUT of the individual replicates.

2.6. Modelling inactivation kinetics

Since the classical concept of D and z values is unable to deal with the typical non-loglinear behaviour of survivor curves during mild thermal treatments, the inactivation model of Geeraerd et al. (2000), able to describe shoulder and tailing behaviour, was fitted to the experimental data obtained on BHI agar (total cell population). Preliminary tests demonstrated that including a shoulder in the model equations would not influence the obtained parameter values. Hence, the factor describing the inactivation shoulder was omitted from the model equations. In order to be suitable for non-isothermal inactivation, the model was extended with a Bigelow-type relation (Garre et al., 2017), using the measured (average) temperature-time profiles inside the respective model system as an input. Model parameters were estimated from the set of experimental data via the minimisation of the sum of squared errors, using the lsqnonlin routine of the Optimisation Toolbox of MatLab® version R2018b (The Mathworks Inc., Natick, USA). For each condition (i.e., one model system and one initial cell condition), the differential equations of the inactivation model were solved simultaneously for the inactivation data at 59, 64 and 69°C, using the MatLab solver ode45. Standard errors of parameter estimates were calculated from the Jacobian matrix. A global estimation procedure was standardised for all replicates for each model system. The model of Geeraerd et al. (2000) is represented by Equations (1), while the Bigelow-type temperature relation is represented by Equation (2).

$$\frac{dN(t)}{dt} = -k_{max}\left(1 - \frac{N_{res}}{N(t)}\right)N(t) \quad (1)$$

$$k_{max}(T) = k_{max}(T_{ref})\,10^{\frac{T-T_{ref}}{z}} \quad (2)$$

With N [CFU/mL], the cell density at time t; N_{res} [CFU/mL], the residual cell density; $k_{\max}$ [1/min], the maximum specific inactivation rate; T [°C], the core-temperature of the model system; T_{ref} [°C], the reference temperature; $k_{max}(T_{ref})$ [1/min], the maximum specific inactivation rate at the reference temperature; and z [−], representing sensitivity of k_{max} to temperature changes. Since *L. monocytogenes* is not inactivated at temperatures lower than 50°C (Valdramidis et al., 2006), k_{max} was assumed to be equal to zero for these temperatures. A reference temperature T_{ref} equal to 64°C was used.

Samples for which cell counts were below the DL were not included in the datasets which were used for model fitting. Due to the disadvantages related to excluding data below the DL from the fitting datasets (e.g., overestimation of cell concentrations, data censoring) and including non-detects as discrete values equal to (a function of) the DL (e.g., model fit which depends on the used function) (Chik et al., 2018), microbiological data were included up until the last time point for which no data below the DL were recorded. Data below the DL were, however, included in the obtained graphs for discussion purposes, representing sample points for which no colonies were detected by a value of 0 log (CFU/mL). At conditions for which the fit was not based on all available data points, N_{res} values were calculated as the average cell density at the last time point to enable a comparison to other conditions.

2.7. Sublethal injury assessment

Sublethal injury (SI) was estimated using Equation (3) (Busch and Donnelly, 1992), using BHI agar and PALCAM agar as a nonselective and selective medium, respectively.

$$SI = \frac{\text{CFU on BHI agar} - \text{CFU on PALCAM agar}}{\text{CFU on BHI agar}}\,100\ [\%] \quad (3)$$

Counts on the nonselective medium represent the total population of injured and uninjured cells, while counts on the selective medium represent the population of injured cells (Noriega et al., 2013). Log-transformed cell densities at the individual time points were used as an input for Equation (3) and SI was assumed to be equal to zero when counts on PALCAM were higher than those on BHI. Furthermore, datapoints for which the counts on BHI were below the DL were omitted.

A third-degree polynomial was fitted to the datapoints calculated from Equation (3), imposing a zero value to replace negative values of the polynomial. The Time-averaged Injured Cells Coefficient (TICC) was calculated using Equation (4) (Miller et al., 2006). The TICC quantifies SI by taking the average of the total SI over the total treatment time for a specific condition.

$$TICC = \frac{\int_0^{t_f} SI(t)dt}{t_f} \quad (4)$$

With t [min], the treatment time; t_f [min], the total duration of the

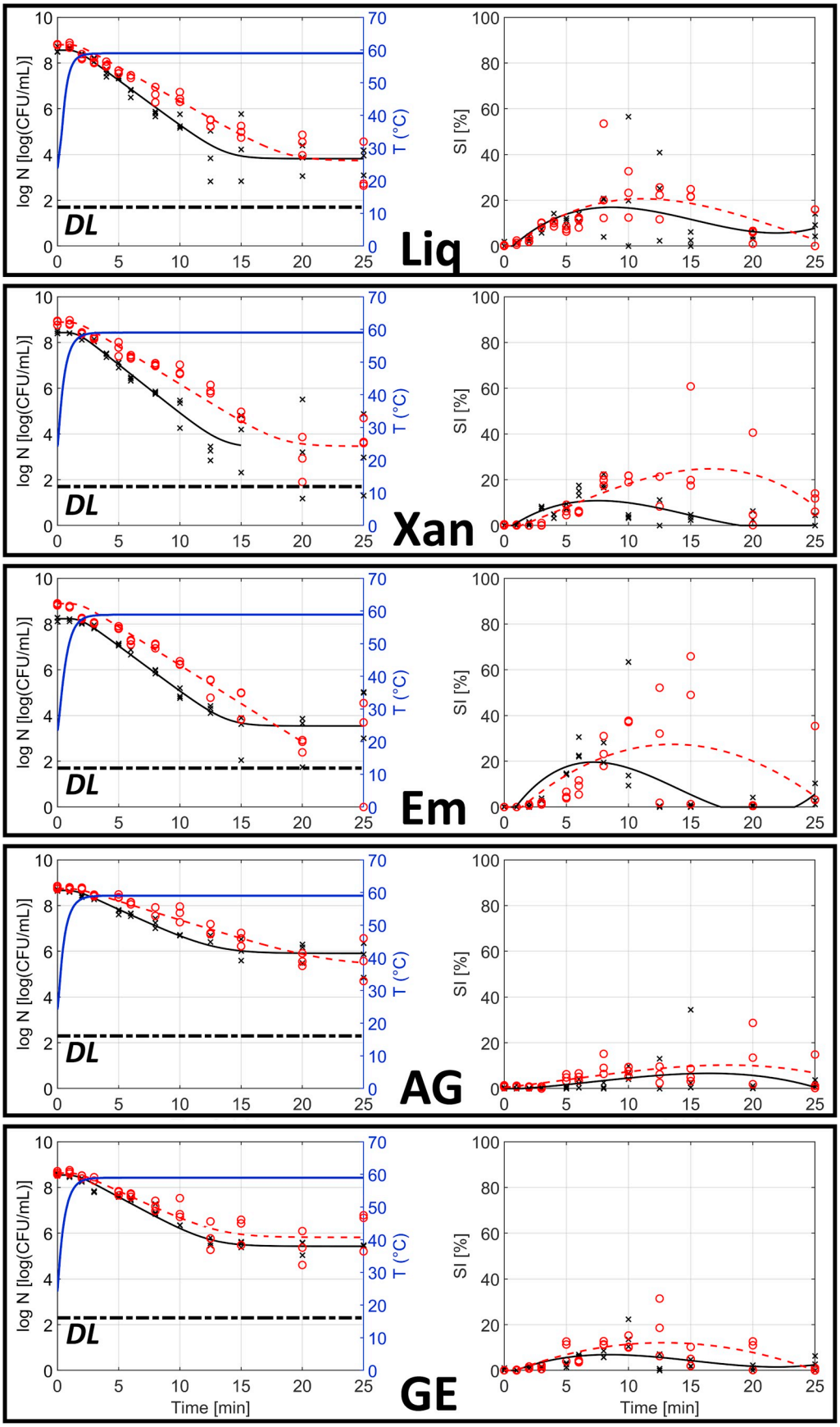

Fig. 2. Inactivation kinetics and sublethal injury (SI) of *L. monocytogenes* at 59°C in the different model systems (Liq = liquid, Xan = xanthan, Em = emulsion, AG = aqueous gel, GE = gelled emulsion). Symbols correspond to the experimental data and lines correspond to the model fit, based on the Geeraerd et al. (2000) model for the inactivation of the total cell population (left), and a third-degree polynomial fitted to the datapoints obtained from Equation (3) for the sublethal injury (SI) (right). The situations where the experiment was started from (i) cells that were grown in the model systems matrix and (ii) cells that were grown at optimal conditions are indicated in red (symbol: o, line: -) and black (symbol: x, line:), respectively. Blue lines represent the temperature evolution in the core of the model system during the thermal treatment. The detection limit (DL) is also indicated on the graphs. (For interpretation of the references to colour in this figure legend, the reader is referred to the Web version of this article.)

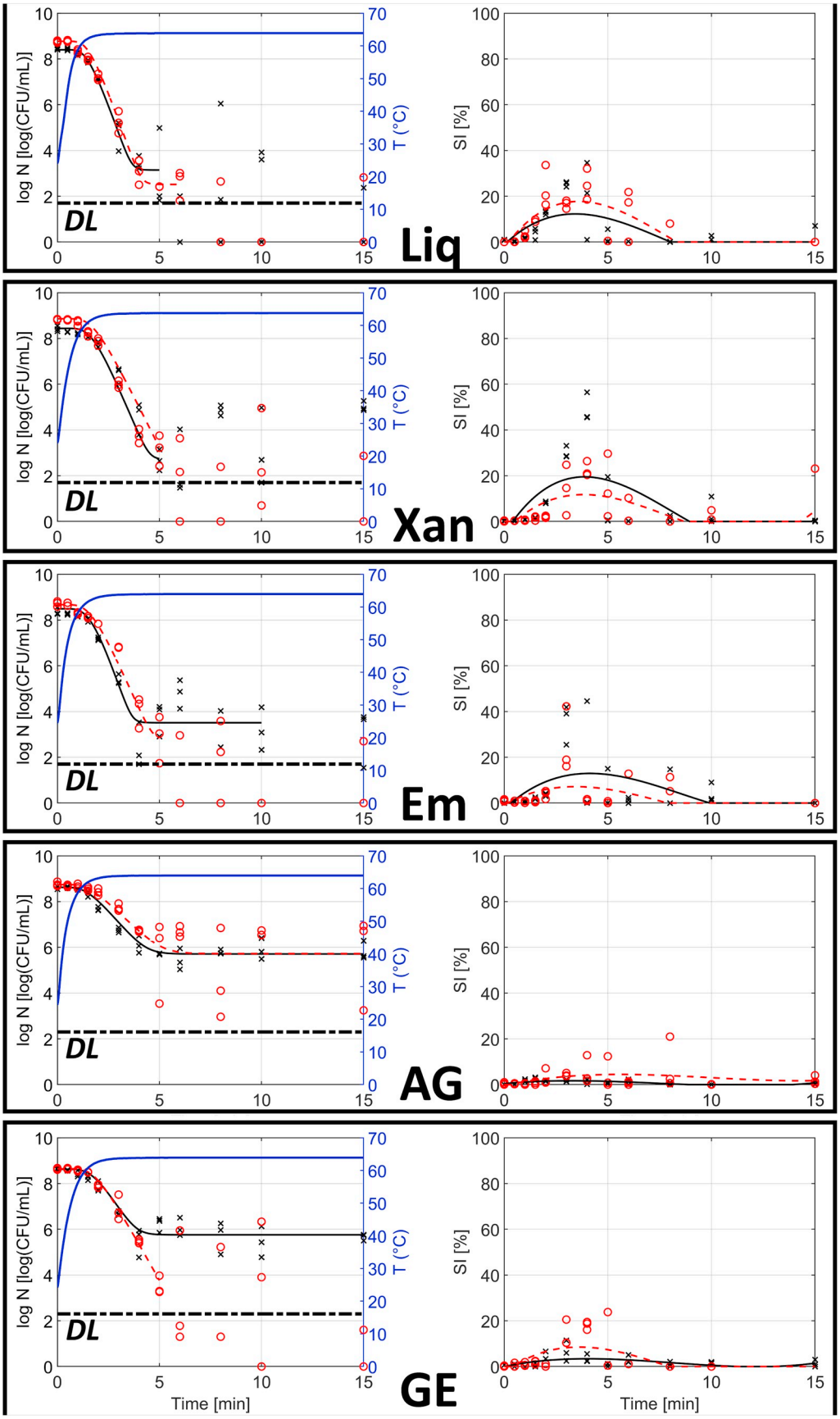

Fig. 3. Inactivation kinetics and sublethal injury (SI) of *L. monocytogenes* at 64°C in the different model systems (Liq = liquid, Xan = xanthan, Em = emulsion, AG = aqueous gel, GE = gelled emulsion). Symbols correspond to the experimental data and lines correspond to the model fit, based on the Geeraerd et al. (2000) model for the inactivation of the total cell population (left), and a third-degree polynomial fitted to the datapoints obtained from Equation (3) for the sublethal injury (SI) (right). The situations where the experiment was started from (i) cells that were grown in the model systems matrix and (ii) cells that were grown at optimal conditions are indicated in red (symbol: o, line: -) and black (symbol: x, line:), respectively. Blue lines represent the temperature evolution in the core of the model system during the thermal treatment. The detection limit (DL) is also indicated on the graphs. (For interpretation of the references to colour in this figure legend, the reader is referred to the Web version of this article.)

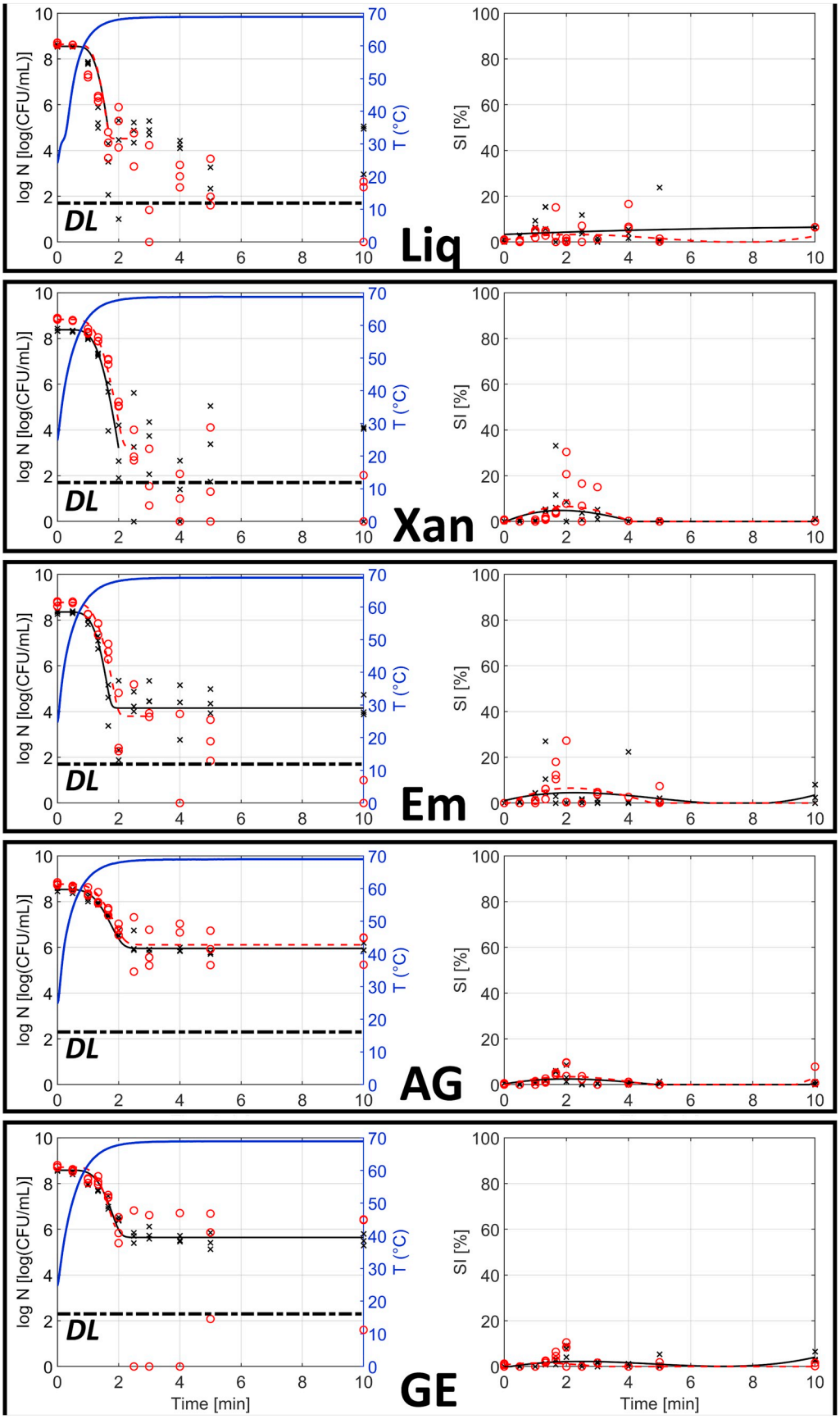

Fig. 4. Inactivation kinetics and sublethal injury (SI) of *L. monocytogenes* at 69°C in the different model systems (Liq = liquid, Xan = xanthan, Em = emulsion, AG = aqueous gel, GE = gelled emulsion). Symbols correspond to the experimental data and lines correspond to the model fit, based on the Geeraerd et al. (2000) model for the inactivation of the total cell population (left), and a third-degree polynomial fitted to the datapoints obtained from Equation (3) for the sublethal injury (SI) (right). The situations where the experiment was started from (i) cells that were grown in the model systems matrix and (ii) cells that were grown at optimal conditions are indicated in red (symbol: o, line: -) and black (symbol: x, line:), respectively. Blue lines represent the temperature evolution in the core of the model system during the thermal treatment. The detection limit (DL) is also indicated on the graphs. (For interpretation of the references to colour in this figure legend, the reader is referred to the Web version of this article.)

thermal treatment; and SI [%], the percentage of sublethal injury at each time point according to the fitted polynomial.

2.8. Statistical analysis

Significant differences between model parameter estimates were determined using analysis of variance (ANOVA, single variance) test at a 95.0% confidence level ($\alpha = 0.05$). Fisher's Least Significant Difference (LSD) test was used to distinguish which means were significantly different from others. The standardised skewness and standardised kurtosis were used to assess if data sets came from normal distributions. The analyses were performed using Statgraphics Centurion 17 Package (Statistical Graphics, Washington, USA). Test statistics were regarded as significant when $P \leq 0.05$.

3. Results and discussion

3.1. Temperature evolution

Figs. 2–4 show the inactivation kinetics (left part of figures) and SI evolution (right part of figures) of *L. monocytogenes* in the different model systems at 59, 64 and 69°C, respectively. Mean Squared Error (MSE) and z values are shown in Table 2. For each condition, a shoulder phase, a log-linear inactivation phase and a tailing phase can be distinguished on the inactivation graphs. The inactivation of *L. monocytogenes* generally started when a core-temperature of approximately 50°C was reached, similar to the minimum inactivation temperature as included in the mathematical model. Since inactivation started when the minimum temperature was reached, the shoulder phase observed for all curves in Figs. 2–4 can be explained by the temperature being lower than the minimum inactivation temperature for *L. monocytogenes*. Hence, there was no typical inactivation shoulder, as interpreted by Geeraerd et al. (2000), i.e., caused by cells being present in groups or clumps, cells being able to resynthesise a vital component, the presence of proteins and/or fats in the medium, or the presence of a large number of critical components that needs to be inactivated (Adams and Moss, 1995; Cerf, 1977; Geeraerd et al., 2000; Moats et al., 1971). Therefore, the influence of microstructural aspects and initial cell conditions on the shoulder phase duration is not further discussed in this study.

While the temperature evolution in each model system is also indicated in Figs. 2–4, Fig. 5 provides a comparison of the temperature evolution in the centre of the different model systems at each specific temperature, as well as the set temperature in the water bath. Temperature evolution is only displayed for the first 4 min of the thermal treatments, after which temperatures remained constant. All model systems showed a temperature profile with a logarithmic shape. The liquid model system was the only exception, exhibiting (at least) one inflection point at each temperature. Since the centre of the model systems was not immediately equal to the temperature of the water bath, a come-up time (CUT) was observed. This CUT was most likely caused by heat transfer limitations throughout the heating medium (Kotrola and Conner, 1997). An overview of the CUT for the different model systems at the different temperatures is provided in Table 3. At 59°C and 64°C, the CUT was the shortest in the liquid model system.

Table 2
z-values and Mean Squared Error (MSE) for the fit to the Geeraerd et al. (2000) model in the different model systems, both for experiments started from cells grown inside the matrix (Mat.) and grown at optimal conditions (Opt.). For each condition, the differential equations were solved simultaneously for the inactivation data at 59, 64, and 69 °C.

	Mat.		Opt.	
	z (°C)	MSE (−)	z (°C)	MSE (−)
Liq.	5.23 ± 0.01	2.03	5.98 ± 0.03	6.01
Xan.	6.40 ± 0.00	1.60	6.72 ± 0.00	1.82
Em.	6.50 ± 0.01	1.44	6.13 ± 0.00	1.89
A.G.	6.88 ± 0.00	1.89	7.90 ± 0.00	0.27
G.E.	6.07 ± 0.00	1.02	7.18 ± 0.01	0.41

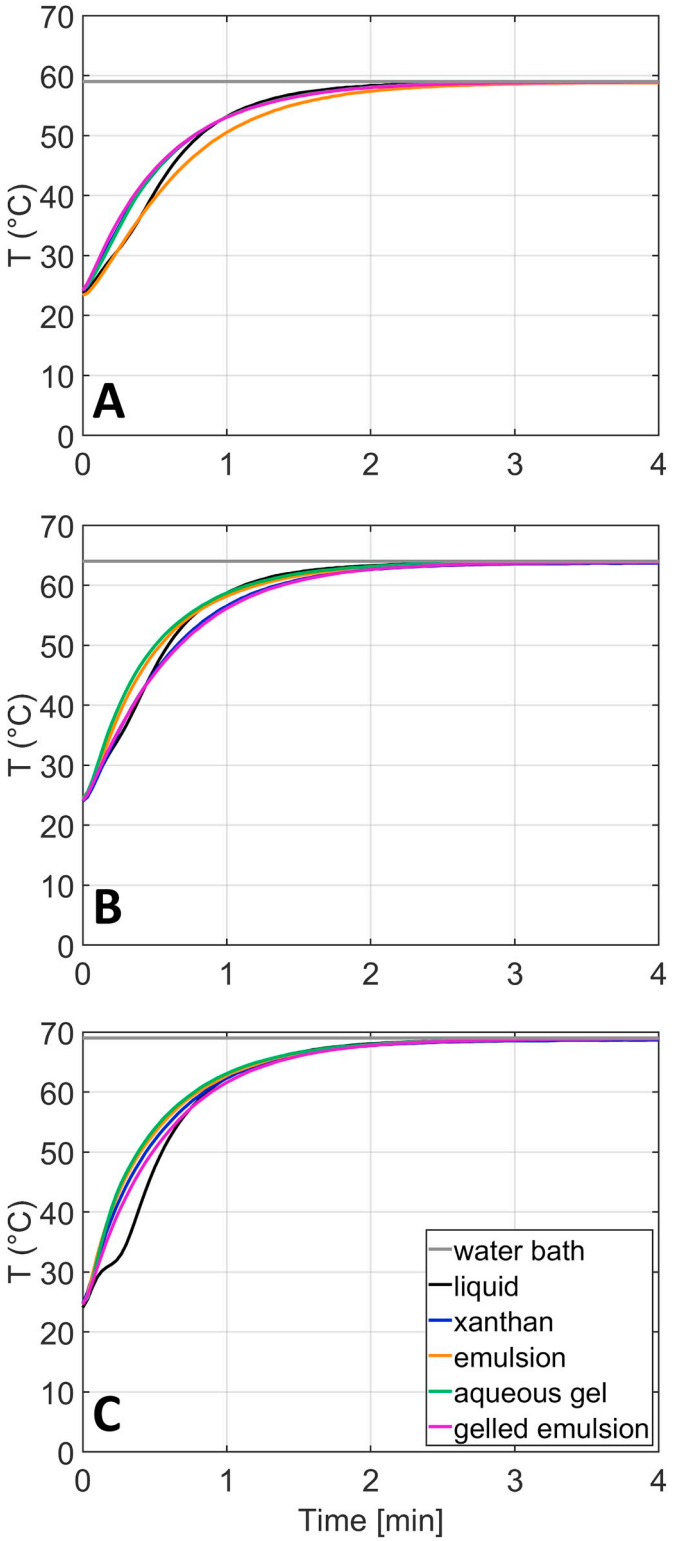

Fig. 5. Temperature evolution in the centre of the different model systems (i.e., liquid, xanthan, emulsion, aqueous gel, and gelled emulsion) and the set temperature in the water bath during the first 4 min of the inactivation experiments at 59°C (A), 64°C (B), and 69°C (C).

Table 3
Come-up time (CUT) in the different model systems for thermal inactivation experiments at 59, 64, and 69°C. For the different model systems (per column) at a certain temperature, values bearing different lowercase letters are significantly different ($P \leq 0.05$).

	CUT (s)		
	59 °C	64 °C	69 °C
liquid	127 ± 8[a]	120 ± 11[a]	130 ± 8[a]
xanthan	134 ± 2[a,b]	141 ± 7[b,c]	128 ± 14[a]
emulsion	150 ± 2[c]	141 ± 6[b,c]	130 ± 10[a]
aqueous gel	138 ± 7[b]	128 ± 10[a,b]	131 ± 12[a]
gelled emulsion	135 ± 3[a,b]	143 ± 3[c]	135 ± 7[a]

This could have been caused by the lower viscosity of the liquid system compared to the other viscous systems (Verheyen et al., 2018a), promoting convective heat transfer. In the gelled systems, convective heat transfer was not possible due to the structural stability of the matrix. At lower temperatures, the thermal conductivity in the liquid system is also significantly higher than in the other (viscous and gelled) systems (Erdogdu et al., 2018), in turn promoting conductive heat transfer. The relationship between the other model systems at these temperatures was more complex, but also corresponded to differences in thermal conductivity among the systems at lower temperatures. At 69°C, no significant differences in CUT were observed, implying that differences in heat transfer rates are less prominent at higher temperatures. Differences in thermal conductivity values among the different model systems at higher temperatures were limited in comparison to lower temperatures (Erdogdu et al., 2018), confirming this hypothesis. These results also suggest that conductive heat transfer was dominant over convective heat transfer in all model systems.

With the small volume of model system (i.e., 1 mL) used for the inactivation experiments, temperature gradients (i.e., core vs. edge) were rather small, reaching approximately 10–15 °C after 20 s treatment, but decreasing rapidly afterwards. CUT in the outer surface layer of the model system was 20–25% lower than at the core (results not shown). Core temperature profiles were used as input for the inactivation model of Geeraerd et al. (2000), since the core temperature is the most relevant for industrial applications.

3.2. Influence of microstructural aspects on thermal inactivation kinetics

The model systems used allow the investigation of three isolated microstructural aspects, as described in more detail in Fig. 6, i.e., (i) growth morphology of the microorganisms, (ii) the nature of the food matrix, and (iii) the presence of fat droplets (Verheyen et al., 2018b). Tables 4–6 provide an overview of the statistical analysis of the parameters of the model of Geeraerd et al. (2000) for the inactivation of *L. monocytogenes* at 59, 64, and 69°C, respectively. For each microstructural aspect, the influence on k_{max} and N_{res} was evaluated based on these tables. The maximum specific inactivation rate k_{max} represents the first order kinetics of the loglinear part of the inactivation curve. The residual cell population N_{res} is related to the tailing part of the inactivation curve. In this regard, N_{res} represents a more resistant subpopulation, originating from adaption phenomena to heat and/or genetic heterogeneity (Geeraerd et al., 2000).

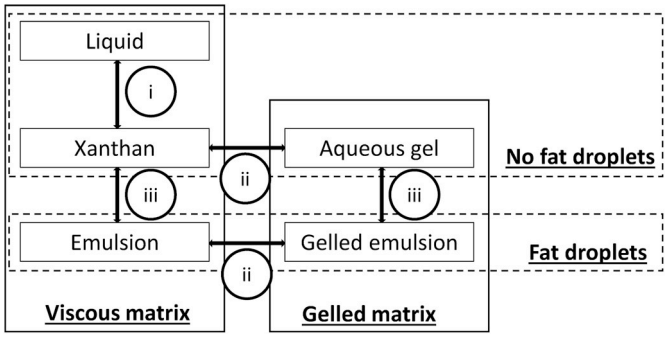

Fig. 6. Schematic overview of the different model systems and their respective microstructural characteristics. The investigation of the microstructural aspects is divided into different aspects, i.e., (i) effect of growth morphology, (ii) effect of the nature of the food matrix, and (iii) the effect of fat droplets (adapted from Verheyen et al., 2018b).

3.2.1. Growth morphology

Growth morphology of *L. monocytogenes* was interpreted as the form of growth (e.g., single cells, colonies) and the colony size (if relevant). Bacteria growing within food products are generally present as single cells or colonies. Bacterial colonies have a minimum radius of 1.5 µm and can be further categorised as micro-colonies (i.e., radius < 100–200 µm) and macro-colonies (i.e., radius > 200 µm). In addition, single cells can also occur as small aggregates (i.e., radius < 1.5 µm); too small to be categorised as micro-colonies (Bae et al., 2011; Choo-Smith et al., 2001; Dos Reis-Teixeira et al., 2017; Jeanson et al., 2015; Zhao et al., 2014).

Since the liquid and xanthan system were the only two systems with no differences in the nature of the food matrix and presence of fat droplets, the influence of bacterial growth morphology on thermal inactivation kinetics could only be systematically studied based on these two. Confocal laser scanning microscopy images of *L. monocytogenes* after 14 days of growth showed that cells in the liquid were mainly present as small aggregates and micro-colonies with a radius between 1.5 and 5.0 µm. In the xanthan system, micro-colonies with a radius between 5.0 and 15.0 µm dominated (Verheyen et al., 2019). Hence, *L. monocytogenes* growth morphology in the liquid and xanthan system was different for experiments started from cells grown inside the matrix. For experiments started from cells grown at optimal conditions, inoculation of the model systems preceded the inactivation experiment by approximately 16 h. It seems rather unlikely that the cells could organize as micro-colonies during this short time period. Therefore, it is assumed that no major differences in *L. monocytogenes* growth morphology between the liquid and xanthan system were present when grown at optimal conditions.

At 59°C (Table 4), the maximum specific inactivation rate k_{max} was significantly higher in the xanthan than in the liquid system, while at 64 (Table 5) and 69°C (Table 6), k_{max} was higher in the liquid than in the xanthan system, and this applied for both initial cell conditions. Since differences in growth morphology between the liquid and xanthan system were identical for the three temperatures prior to the inactivation experiment, significant differences in k_{max} could not be caused by differences in growth morphology. Alternatively, the treatment temperature could have exerted an influence on the thermotolerance of *L. monocytogenes*. Fig. 5 showed that differences in core-temperature evolution between the liquid and xanthan system were not equal at the three temperatures. The influence could therefore be related to a different influence of temperature on the thermal conductivity and viscosity of the liquid and xanthan system and resulting conductive and convective heat transfer differences between the two systems. Differences in conductive heat transfer between the two systems were more prominent at lower temperatures, as discussed in more detail in Section 3.1 "Temperature evolution". Concerning convective heat transfer, the viscosity of the xanthan system is significantly higher than that of the liquid system. In addition, the liquid system exhibits Newtonian behaviour, while the xanthan system exhibits non-Newtonian pseudo-plastic behaviour (Verheyen et al., 2018a). Viscosity measurements of the two systems at different temperatures demonstrated that the viscosity of the xanthan system was reduced by approximately 50% when the temperature was increased from 59 to 69°C, while the viscosity of the liquid was only reduced by approximately 10% (results not shown). These thermal and rheological characteristics of the model systems could be

Table 4
Parameter estimation and statistical analysis of the maximum specific inactivation rate k_{max} and the residual cell density N_{res}, according to the inactivation model of Geeraerd et al. (2000) for the thermal inactivation of *L. monocytogenes* in the five model systems (Liq. = liquid, Xan. = xanthan, Em. = emulsion, A.G. = aqueous gel, and G.E. = gelled emulsion) at 59°C, enumerated on BHI agar. Experiments were either started from cells that were grown inside the matrix (Mat.) or grown at optimal conditions (Opt.). For the different initial conditions for one model system, values bearing different lowercase letters are significantly different ($P \leq 0.05$). For the different model systems with the same initial condition, values bearing different uppercase letters are significantly different ($P \leq 0.05$).

	k_{max} (1/min)		N_{res} (log (CFU/mL))	
	Mat.	Opt.	Mat.	Opt.
Liq.	0.299 ± 0.001 (a,C)	0.394 ± 0.004 (b,C)	3.73 ± 0.01 (a,AB)	3.82 ± 0.01 (a,A)
Xan.	0.325 ± 0.000 (a,D)	0.421 ± 0.001 (b,E)	3.46 ± 0.00 (a,AB)	3.05 ± 1.79 (a,A)[a]
Em.	0.352 ± 0.000 (a,E)	0.417 ± 0.000 (b,D)	2.75 ± 2.42 (a,A)[a]	3.54 ± 0.01 (a,A)
A.G.	0.165 ± 0.000 (a,A)	0.246 ± 0.000 (b,A)	5.38 ± 0.03 (a,BC)	5.91 ± 0.00 (b,B)
G.E.	0.249 ± 0.000 (a,B)	0.292 ± 0.000 (b,B)	6.22 ± 0.88 (a,C)[a]	5.43 ± 0.00 (a,B)

[a] N_{res} calculated as the average cell density at the final time point.

an explanation for the observed inactivation phenomena, even though more research is needed to further elucidate the specific mechanisms of interest (i.e., influence of thermal conductivity and product viscosity on heat transfer and inactivation kinetics). Concerning the residual cell population N_{res}, no significant differences were observed between the liquid and xanthan system for both initial cell conditions, with the inactivation at 64°C started from cells grown at optimal conditions as the only exception to this observation (i.e., N_{res} higher in xanthan). Hence it can be assumed that differences in *L. monocytogenes* growth morphology between the liquid and xanthan system (i.e., caused by differences in microstructural aspects among the two systems rather than by differences in initial cell conditions) do not exert a significant influence on thermal inactivation kinetics.

Regarding the influence of growth morphology on microbial growth dynamics, Verheyen et al. (2018b) demonstrated that the maximum specific growth rate of *L. monocytogenes* at 10 °C in the liquid system was significantly lower than in the xanthan system. This phenomenon was most probably caused by the greater oxygen availability in the xanthan system, as cells in the liquid system sedimented to the bottom of the tubes due to static conditions (Verheyen et al., 2018b). Since k_{max} in the liquid system was not consistently lower than in the xanthan system at all temperatures, it can be assumed that the stress induced to the cells by the limited oxygen availability in the liquid system does not induce considerable cross-protective effects against thermal treatments.

As previously explained, it was in the current study not possible to investigate the effect of *L. monocytogenes* growth morphology on thermal inactivation kinetics in the emulsion, aqueous gel, and gelled emulsion model system. This effect could be elucidated in further studies, for example by developing model systems with different rheological properties to acquire different growth morphologies (preferably confirmed by microscopic images) in the systems prior to thermal inactivation.

3.2.2. Nature of the food matrix

The effect of the food matrix on the inactivation kinetics of *L. monocytogenes* is studied by means of the effect of the presence of a gelled matrix, i.e., aqueous gel vs. xanthan and gelled emulsion vs. emulsion.

For all inactivation temperatures, it was observed that the maximum specific inactivation rate k_{max} in the viscous system was significantly higher than in the respective gelled system. The residual cell population N_{res} in the viscous system was significantly lower than or equal to N_{res} in the respective gelled system. Since the residual cell population N_{res} also relates to the log-reduction caused by the thermal treatments, the higher N_{res} values in gelled systems are especially interesting. A protective effect of a gelled matrix against thermal inactivation was present, albeit dependent on the initial cell conditions and the inactivation temperature. It has been reported that bacterial cells which are surrounded by a gelled matrix might experience alterations in cell development, membrane permeability, surface tension, osmotic pressure and metabolism, potentially affecting their thermal resistance (Dervakos and Webb, 1991; Meldrum et al., 2003; Noriega et al., 2013; Wilson et al., 2002). In section 3.2.1 "Growth morphology", it was already determined that the effect of the growth morphology of *L. monocytogenes* on thermal inactivation kinetics was not significant in the current study. Consequently, the higher heat resistance which has often been observed for submerged colonies in a gelled environment as compared to planktonic cells in broth systems (Murphy et al., 2000; Velliou et al., 2013), is probably also caused by a protective effect of the gelled environment and not by the differences in growth morphology.

Considering the case were cells were grown inside the model system matrix, Verheyen et al. (2018b) demonstrated that *L. monocytogenes* growth at 10 °C in the same set of model systems was more pronounced (i.e., higher maximum specific growth rate) in a viscous matrix than in a gelled matrix, suggesting that cells in a gelled matrix are subjected to

Table 5
Parameter estimation and statistical analysis of the maximum specific inactivation rate k_{max} and the residual cell density N_{res}, according to the inactivation model of Geeraerd et al. (2000) for the thermal inactivation of *L. monocytogenes* in the five model systems (Liq. = liquid, Xan. = xanthan, Em. = emulsion, A.G. = aqueous gel, and G.E. = gelled emulsion) at 64°C, enumerated on BHI agar. Experiments were either started from cells that were grown inside the matrix (Mat.) or grown at optimal conditions (Opt.). For the different starting conditions for one model system, values bearing different lowercase letters are significantly different ($P \leq 0.05$). For the different model systems with the same initial condition, values bearing different uppercase letters are significantly different ($P \leq 0.05$).

	k_{max} (1/min)		N_{res} (log (CFU/mL))	
	Mat.	Opt.	Mat.	Opt.
Liq.	2.70 ± 0.01 (a,E)	2.70 ± 0.00 (a,D)	0.94 ± 1.63 (a,A)[a]	0.79 ± 1.63 (a,A)[a]
Xan.	1.96 ± 0.00 (a,C)	2.33 ± 0.01 (b,C)	0.96 ± 1.65 (a,A)[a]	5.02 ± 0.22 (b,C)[a]
Em.	2.07 ± 0.00 (a,D)	2.70 ± 0.00 (b,D)	0.90 ± 1.56 (a,A)[a]	2.98 ± 1.25 (a,B)[a]
A.G.	0.88 ± 0.00 (a,A)	1.06 ± 0.00 (b,A)	5.72 ± 0.01 (a,B)	5.71 ± 0.01 (a,C)
G.E.	1.66 ± 0.00 (b,B)	1.45 ± 0.00 (a,B)	0.53 ± 0.92 (a,A)[a]	5.76 ± 0.00 (b,C)

[a] N_{res} calculated as the average cell density at the final time point.

Table 6
Parameter estimation and statistical analysis of the maximum specific inactivation rate k_{max} and the residual cell density N_{res}, according to the inactivation model of Geeraerd et al. (2000) for the thermal inactivation of *L. monocytogenes* in the five model systems (Liq. = liquid, Xan. = xanthan, Em. = emulsion, A.G. = aqueous gel, and G.E. = gelled emulsion) at 69°C, enumerated on BHI agar. Experiments were either started from cells that were grown inside the matrix (Mat.) or grown at optimal conditions (Opt.). For the different starting conditions for one model system, values bearing different lowercase letters are significantly different ($P \leq 0.05$). For the different model systems with the same initial condition, values bearing different uppercase letters are significantly different ($P \leq 0.05$).

	k_{max} (1/min)		N_{res} (log (CFU/mL))	
	Mat.	Opt.	Mat.	Opt.
Liq.	24.4 ± 0.2 (b,E)	18.5 ± 0.2 (a,E)	1.68 ± 1.46 (a,A)[a]	4.32 ± 1.18 (a,AB)[a]
Xan.	11.8 ± 0.0 (a,C)	13.0 ± 0.0 (b,C)	0.67 ± 1.17 (a,A)[a]	2.72 ± 2.36 (a,A)[a]
Em.	12.2 ± 0.0 (a,D)	17.5 ± 0.0 (b,D)	0.33 ± 0.58 (a,A)[a]	4.15 ± 0.00 (b,AB)
A.G.	4.70 ± 0.01 (b,A)	4.55 ± 0.00 (a,A)	6.11 ± 0.05 (b,B)	5.95 ± 0.00 (a,B)
G.E.	11.1 ± 0.0 (b,B)	7.21 ± 0.01 (a,B)	4.81 ± 2.78 (a,B)[a]	5.64 ± 0.00 (a,B)

[a] N_{res} calculated as the average cell density at the final time point.

more stressing conditions. These stressing conditions might lead to an increased resistance to a subsequent thermal treatment. For example, the cells could become more heat resistant after growth in the gelled matrix due to a cross-protective effect caused by an acid tolerance response triggered by the local accumulation of acidic metabolites (Noriega et al., 2013; Malakar et al., 2000; Walker et al., 1997; Wilson et al., 2002).

Future predictive models that aim to incorporate the influence of food microstructure on thermal inactivation kinetics of foodborne pathogens could therefore benefit from the inclusion of a factor that describes the influence of the nature of the food matrix. To this extent, the effect on thermal inactivation kinetics of the rheological and structural parameters, which were already determined for the current set of model systems in Verheyen et al. (2018a), could be investigated, i.e., viscosity parameters of the Power law model (Reiner, 1926) for viscous systems, and the storage (G') and loss (G") modulus for gelled systems.

3.2.3. Presence of fat droplets

The influence of the presence of fat droplets on the thermal inactivation of *L. monocytogenes* is studied by comparing inactivation kinetics between systems where the presence of a small amount (i.e., 1% fat content) of fat droplets is the only distinguishing factor, i.e., xanthan vs. emulsion and aqueous gel vs. gelled emulsion. Since the small amount of fat droplets had no influence on the pH and a_w of the model systems (Verheyen et al., 2018a), differences in microbial kinetics were only caused by the presence of the fat droplets.

For both initial cell conditions at the three temperatures, the maximum specific inactivation rate k_{max} in the systems containing fat droplets was always significantly higher than in the respective systems without fat droplets. The only exception to this observation occurred between the xanthan and emulsion system at 59°C for experiments started from cells grown at optimal conditions, where k_{max} was significantly lower in the emulsion system than in the xanthan system. The exact explanation for this exception remains unclear, but it should be noted that the difference between the two k_{max} values was rather small. Using emulsion systems with higher fat content, which did not fit in the scope of the current study due to the need for limited compositional differences, could lead to clearer differences. Concerning the residual cell population N_{res}, no statistical differences were observed between systems with and without fat droplets in most cases. At 64°C, however, N_{res} was significantly lower in systems containing fat droplets at two conditions, i.e., xanthan vs. emulsion for cells grown at optimal conditions and aqueous gel vs. gelled emulsion for cells grown inside the matrix. Hence, it can be concluded that the presence of fat droplets in the food matrix leads to a reduced thermotolerance of *L. monocytogenes*, always significantly increasing k_{max}, while only significantly reducing N_{res} in some conditions. In this regard, Verheyen et al. (2018b) already established a growth-promoting effect of the presence of fat droplets (i.e., small fat concentration of 1%) on *L. monocytogenes* at 4 °C, suggesting that growth at more stressing conditions leads to an increased resistance to a subsequent thermal treatment, similar to what was previously reported concerning the influence of the nature of the food matrix.

In order to acquire more insight into the exact influencing mechanisms of the presence of fat droplets on thermal inactivation kinetics, the influence of fat concentration and fat droplet size distribution could be investigated. To the best knowledge of the authors, no studies have been conducted on the influence of fat droplet size distribution on thermal inactivation kinetics so far. Previous studies on the influence of different fat concentration levels on thermal inactivation kinetics, on the other hand, do not show consistent results. The thermotolerance of bacteria (i.e., *Listeria* or *Salmonella*) either increased (Chhabra et al., 1999; Fain et al., 1991; Juneja et al., 2001) or decreased (Schultze et al., 2007), or was not significantly affected (Passos and Kuaye, 2002; Szlachta et al., 2010) by increasing the fat concentration of the heating medium. These studies, however, were conducted in real food products (*e.g.*, milk, ground beef, ground poultry, frankfurters) and with different bacterial strains. Thermal inactivation kinetics could therefore also have been influenced by variations in compositional (e.g., salt, preservatives), physicochemical factors (*e.g.*, pH, water activity), and strain variability. Future inactivation studies conducted in food model systems with different fat levels or fat droplet size distributions, with minimal variations in compositional and physicochemical factors, could lead to more consistent results. Possibly, such studies would also result in more consistent statistical differences than those observed in the current study.

3.3. Influence of initial cell conditions on thermal inactivation kinetics

It was assessed whether the classical and simplified microbiological method of inoculating food products with cells grown at optimal conditions for challenge testing purposes has sufficient practical relevance. A comparison was made between inactivation starting (i) from cells grown inside the model system matrix (i.e., novel approach) and (ii) from cells grown at optimal conditions (i.e., traditional approach) (see Fig. 1). Therefore, the statistical analysis of k_{max} and N_{res} in Tables 4–6 (at 59, 64 and 69°C, respectively) was used to investigate the influence of the initial cell conditions on inactivation kinetics of *L. monocytogenes*.

At 59°C, cells grown inside the matrix always exhibited a smaller k_{max} than those grown at optimal conditions. At 64°C, the same trend was observed in the xanthan system, the emulsion and the aqueous gel. In the gelled emulsion, k_{max} was smaller when cells were grown at optimal conditions, while in the liquid, no significant differences were observed. At 69°C, k_{max} was smaller when cells were grown inside the matrix in the xanthan and emulsion system, while k_{max} was smaller when cells were grown at optimal conditions in the liquid, aqueous gel and gelled emulsion. Different possible explanations exist for the cases where k_{max} is smaller for cells that were grown inside the matrix, i.e.,

Table 7
Time-averaged Injured Cells Coefficient (TICC) of *L. monocytogenes* for thermal inactivation experiments at 59, 64, and 69°C in the different model systems, both for experiments that were started from cells that were grown inside the matrix (Mat.) and experiments that were started from cells grown at optimal conditions (Opt.).

	59 °C		64 °C		69 °C	
	Mat.	Opt.	Mat.	Opt.	Mat.	Opt.
Liquid	13.5	10.5	6.2	4.2	1.6	5.2
Xanthan	15.7	4.9	4.2	7.1	1.6	1.3
Emulsion	17.9	8.2	2.4	5.3	2.0	2.1
Aqueous gel	7.0	3.9	2.9	0.7	1.1	0.8
Gelled emulsion	7.8	3.9	2.8	1.6	0.3	1.2

the influence of the growth conditions prior to the thermal treatment and differences in colony size. Concerning the influence of the growth conditions, it has been reported that *L. monocytogenes* heat resistance is enhanced when cells are exposed to more stressing growth conditions (Donnelly et al., 1987; Edelson-Mammel et al., 2005), as previously discussed for the influence of the nature of the food matrix and the presence of fat droplets. Concerning differences in colony size, Velliou et al. (2013) reported that starting growth from a higher cell number (i.e., $> 10^3$ CFU/mL) results in a large number of small colonies, while starting from a lower cell number (i.e., $< 10^3$ CFU/mL) results in a smaller number of large colonies. In the present study, larger colonies were therefore obtained in the case where cells were grown inside the food matrix starting from a low cell level than in the case where cells were grown at optimal conditions and inoculated at a high cell density, as confirmed microscopically by Verheyen et al. (2019). Since neighbouring cells can have a protective effect on cells subjected to heat treatments (Adams and Moss, 1995; Geeraerd et al., 2000; Moats et al., 1971), these larger colonies could exhibit an enhanced heat resistance due to the higher number of cells that protect each other inside the colony. In this regard, Noriega et al. (2013) also observed that large colonies of *Listeria innocua* were more heat resistant than smaller colonies when subjected to a mild thermal treatment of 54 °C. A similar effect could be created when cells sediment to the bottom of the tube if grown for 14 days in the liquid system and therefore are situated closer to each other than when inoculated 16 h prior to the inactivation experiment. For the cases where k_{max} was smaller when cells were grown at optimal conditions, it should be noted that this trend was mainly seen for the inactivation experiments at 69°C. In all model systems, the majority of the inactivation of *L. monocytogenes* took place at temperatures which were significantly lower than 69°C, as can be seen in Fig. 4. Therefore, k_{max} values which are presented in Table 6 are mostly theoretical values calculated based on k_{max} values at the reference temperature of 64°C. Since the inactivation model used in the current study was in fact not fitted to inactivation data at 69°C, conclusions based on the calculated k_{max} values at this temperature do not represent significant practical relevance (i.e., extrapolation outside of the experimental domain) and should be interpreted with caution.

In most conditions, no significant differences in N_{res} were observed between the two initial cell conditions. In a majority of the exceptions to this observation (i.e., xanthan and gelled emulsion at 64 °C, emulsion at 69 °C), these statistical differences were caused by the large variation in cell densities of the different biological replicates when cells were grown in the model system matrix. While there were significant differences in cell densities at the final sampling point at which N_{res} was calculated, these differences were not present at earlier sampling points which were also located in the tailing phase. For the other exceptions (i.e., aqueous gel at 59 and 69 °C), the difference in N_{res} between the two initial cell conditions was rather small compared to the other conditions, and measured cell densities at the final sampling point were not significantly different.

Taking into account the lower k_{max} when cells are grown inside the model system matrix, it might be unsafe to employ the common experimental approach of using cells grown at optimal conditions for mild thermal inactivation studies with *L. monocytogenes*. Nevertheless, the current study indicated that starting experiments from cells grown inside the model system matrix also entails disadvantages. A small difference in growth behaviour can result in large variations in heat resistance of the cells, resulting in an increased uncertainty concerning the obtained log reductions. Consequently, researchers should select the appropriate inoculation method for their specific application when designing thermal inactivation experiments. Starting experiments from cells grown at optimal conditions results is more suitable to estimate log reductions, while starting from cells grown inside the food matrix is a more fail-safe approach to estimate k_{max} values.

3.4. Sublethal injury assessment

In Figs. 2–4 (right part of the figures), it can be observed that SI was higher at lower inactivation temperatures. The same observation can be made in Table 7, which provides an overview of the TICC-values for the different model systems during the different thermal treatments. This trend is in accordance with other studies which reported high levels of SI when bacteria were subjected to mild thermal treatments (Miller et al., 2006; Suo et al., 2012; Wuytack et al., 2003). Therefore, this section focused on the experiments at 59°C to discuss SI. At 64 and 69°C, SI was almost absent in some cases, meaning that comparing TICC based on model fit values would probably be inaccurate. In general, a peak in SI coincided with the loglinear inactivation phase of *L. monocytogenes* for all model systems at 59°C. This is in accordance with the findings of Noriega et al. (2013) for the mild heating of *Escherichia coli*, *Salmonella* Typhimurium, and *Listeria innocua* in liquid and gelled model systems. This behaviour during the loglinear inactivation phase is caused by a mechanism of injury accumulation that culminates in cell death (Perni et al., 2007).

3.4.1. Influence of microstructural aspects on sublethal injury

At 59°C (as observed in Fig. 2), SI for all conditions ranged between 0 and 10% at the end of the inactivation treatment. Table 7 illustrates that the TICC was higher in the viscous systems (i.e., liquid, xanthan, emulsion) than in the gelled systems (i.e., aqueous gel, gelled emulsion). This finding confirms the conclusions from section 3.2.2 "Nature of the food matrix", where a protective effect of a gelled matrix against thermal treatments was already determined. For conditions corresponding to the liquid system in the case where cells were grown at optimal conditions, findings of the current study are in accordance with those of previous studies. Uyttendaele et al. (2008) found that the SI of fifteen different *L. monocytogenes* strains after heat treatment at 60°C for 20 min reached a maximum of 60%, calculated based on untransformed cell densities. These values correspond to a SI lower than 15% when calculated based on log-transformed cell densities, the method which was applied in the current study. Similarly, Wang et al. (2017) observed a SI lower than 15% (i.e., 61.8% when calculated based on untransformed cell densities) for *L. monocytogenes* cells which were grown at optimal conditions (i.e., systems were inoculated to a high cell level directly from a preculture which was grown at optimal conditions) and heat treated at 60°C for 10 min. To the best knowledge of the authors, no assessment of SI has been conducted for thermal inactivation of *L. monocytogenes* in model systems which represent the same microstructural spectrum as those from the present study, but results can be compared to some extent with studies which investigated the influence of similar microstructural aspects. Wang et al. (2017) observed higher SI for surface colonies inactivated on agar surface than for planktonic cells inactivated in liquid medium, while Noriega et al. (2013) observed similar SI for submerged colonies in a gelled medium as for planktonic cells in a liquid medium for conditions similar to those from the present study.

3.4.2. Influence of initial cell conditions on sublethal injury

In order to investigate the influence of the initial conditions of the cells on SI induced by the thermal treatment, results for cells grown at optimal conditions were compared to results for cells grown inside the model system. For all model systems at 59°C, the TICC was higher for cells grown inside the food matrix than for cells grown at optimal conditions. In other words, more SI was present when cells were grown inside the model systems. This phenomenon can possibly be explained by the adaption of the cells to their stressing environment while growing inside the matrix (Tang et al., 2015), leading to cross-protection against other stresses (Durack et al., 2013; Lou and Yousef, 1996). Consequently, the cells which have experienced more severe stress responses during the growth phase (due to e.g., cell immobilisation, reduced nutrient availability) might become only sublethally injured by treatments which would completely inactivate cells grown at optimal conditions. This assumption is confirmed by the lower k_{max} values which were obtained for cells grown inside the model system matrix, indicating that cells were inactivated at a lower rate.

4. Conclusions

Thermal inactivation kinetics of *L. monocytogenes* are significantly influenced by food microstructure. This study illustrated that the nature of the food matrix (i.e., viscous or gelled) and the presence/absence of fat droplets influenced the thermal inactivation parameters, i.e., the maximum specific inactivation rate $k_{\max}$ and the residual cell population N_{res}. A protective effect of a gelled matrix against thermal inactivation of *L. monocytogenes*, which was dependent on the initial cell conditions and the inactivation temperature, has been demonstrated. This influence of the nature of the food matrix could be incorporated in future predictive thermal inactivation models by including a "food matrix factor" related to the rheological and/or structural properties of the food product. The presence of fat droplets in the model system matrix, on the other hand, decreased the thermotolerance of *L. monocytogenes*. More research on the effect of fat concentration and/or fat droplet size distributions on thermal inactivation kinetics is necessary for the inclusion of this effect in predictive models. The cell conditions prior to the mild thermal inactivation treatment also exerted a significant influence on microbial inactivation kinetics of *L. monocytogenes*, meaning that researchers need to carefully consider how to inoculate their foods/model systems when conducting thermal inactivation trials. Starting experiments from cells grown inside the model system matrix leads to fail-safe predictions of inactivation rates, while starting from cells grown at optimal conditions reduces uncertainty on predicted log reductions. In addition, SI of *L. monocytogenes* was proven to be an important issue when using milder thermal treatments, with the amount of SI being influenced by the initial conditions of the cells and the nature of the food matrix.

In future studies, a more detailed knowledge of the exact influencing mechanisms of the investigated microstructural aspects could be achieved by conducting thermal inactivation experiments in model systems with varying rheological properties, fat levels and/or fat droplet size distributions. In those studies, one factor should be isolated at a time, while still minimising differences in physicochemical properties. In general, it should also be noted that, even though the used set of model systems simulates processed fish products, applicability to real fish products at industrial conditions could be limited. This issue could also be addressed in future studies by means of a validation step in real food products.

Declarations of interest

None.

Acknowledgements

This work was supported by the Norconserv Foundation, FWO Vlaanderen (grant G.0863.18) and the KU Leuven Research Fund (Center of Excellence OPTEC-Optimization in Engineering and project C24/18/046). Authors Maria Baka and Simen Akkermans were supported by the research council of KU Leuven for post-doctoral researchers (grants PDM/16/125 and PDM/18/136).

References

Adams, M.R., Moss, M.O., 1995. Food Microbiology. Royal Society of Chemistry, Cambridge.
Aguilera, J.M., 2009. Food microstructure. In: In: Barbosa-Cánovas, G.V. (Ed.), Food Engineering, vol. 1. Eolss Publishers Co. Ltd, Oxford (UK), pp. 223–239.
Álvarez-Ordóñez, A., Fernández, A., López, M., Arenas, R., Bernardo, A., 2008. Modifications in membrane fatty acid composition of *Salmonella* typhimurium in response to growth conditions and their effect on heat resistance. Int. J. Food Microbiol. 123, 212–219.
Annous, B.A., Kozempel, M.F., Kurantz, M.J., 1999. Changes in membrane fatty acid composition of *Pediococcus* sp. strain NRRL B-2354 in response to growth conditions and its effect on thermal resistance. Appl. Environ. Microbiol. 65, 2857–2862.
Aryani, D.C., den Besten, H.M.W., Hazeleger, W.C., Zwietering, M.H., 2015. Quantifying variability on thermal resistance of *Listeria monocytogenes*. Int. J. Food Microbiol. 193, 130–138.
Ates, B.M., Skipnes, D., Rode, T.M., Lekang, O., 2014. Comparison of bacterial inactivation with novel agitating retort and static retort after mild heat treatments. Food Bioprocess Technol. 4 (6), 833–848.
Bae, E., Bai, N., Aroonnual, A., Bhunia, A.K., Hirleman, E.D., 2011. Label-free identification of bacterial microcolonies via elastic scattering. Biotechnol. Bioeng. 108, 637–644.
Baka, M., Noriega, E., Tsakali, E., Van Impe, J.F., 2015. Influence of composition and processing of Frankfurter sausages on the growth dynamics of *Listeria monocytogenes* under vacuum. Food Res. Int. 70, 94–100.
Baka, M., Noriega, E., Van Langendonck, K., Van Impe, J.F., 2016. Influence of food intrinsic complexity on *Listeria monocytogenes* growth in/on vacuum-packed model systems at suboptimal temperatures. Int. J. Food Microbiol. 235, 17–27.
Baka, M., Vercruyssen, S., Cornette, N., Van Impe, J.F., 2017a. Dynamics of *Listeria monocytogenes* at suboptimal temperatures in/on fish-protein based model systems: effect of (micro)structure and microbial distribution. Food Control 73, 43–50.
Baka, M., Verheyen, D., Cornette, N., Vercruyssen, S., Van Impe, J.F., 2017b. *Salmonella* Typhimurium and *Staphylococcus aureus* dynamics in/on variable (micro)structures of fish-based model systems at suboptimal temperatures. Int. J. Food Microbiol. 240, 32–39.
Bellara, S.R., Fryer, P.J., McFarlane, C.M., Thomas, C.R., Hocking, P.M., Mackey, B.M., 1999. Visualization and modelling of the thermal inactivation of bacteria in a model food. Appl. Environ. Microbiol. 65, 3095–3099.
Bellara, S.R., McFarlane, C.M., Thomas, C.R., Fryer, P.J., 2000. The growth of *Escherichia coli* in a food simulant during conduction cooling: combining engineering and microbiological modelling. Chem. Eng. Sci. 55, 6085–6095.
Ben Embarek, P.K., 1994. Presence, detection and growth of *Listeria monocytogenes* in seafoods: a review. Int. J. Food Microbiol. 23, 17–34.
Besse, N.G., 2002. Influence of various environmental parameters and of detection procedures on the recovery of stressed *L. monocytogenes*: a review. Food Microbiol. 19, 221–234.
Brashears, M.M., Amezquita, A., Stratton, J., 2001. Validation of methods used to recover *Escherichia coli* O157:H7 and *Salmonella* spp. subjected to stress conditions. J. Food Prot. 64 (10), 1466–1471.
Busch, S.V., Donnelly, C.W., 1992. Development of a repair-enrichment broth for resuscitation of heat-injured *Listeria monocytogenes* and *Listeria innocua*. Appl. Environ. Microbiol. 58, 14–20.
Cerf, O., 1977. A review. Tailing of survival curves of bacterial spores. J. Appl. Bacteriol. 42 (1), 1–19.
Chik, A.H.S., Schmidt, P.J., Emelko, M.B., 2018. Learning something from nothing: the critical importance of rethinking microbial non-detects. Front. Microbiol. 9, 2304.
Chhabra, A.T., Carter, W.H., Linton, R.H., Cousin, M.A., 1999. A predictive model to determine the effects of pH, milkfat, and temperature on thermal inactivation of *Listeria monocytogenes*. J. Food Prot. 62, 1143–1149.
Choo-Smith, L.P., Maquelin, K., van Vreeswijk, T., Bruining, H.A., Puppels, G.J., Ngo Thi, N.A., Kirschner, C., Naumann, D., Ami, D., Villa, A.M., Orsini, F., Doglia, S.M., Lamfarraj, H., Sockalingum, G.D., Manfait, M., Allouch, P., Endtz, H.P., 2001. Investigating microbial (micro)colony heterogenity by vibrational spectroscopy. Appl. Environ. Microbiol. 67 (4), 1461–1469.
Chung, H.-J., Birla, S.L., Tang, J., 2008. Performance evaluation of aluminum test cell designed for determining the heat resistance of bacterial spores in foods. LWT 41, 1351–1359.
Dervakos, G.A., Webb, C., 1991. On the merits of viable-cell immobilisation. Biotechnol. Adv. 9 (4), 559–612.
Devlieghere, F., Vermeiren, L., Debevere, J., 2004. New preservation technologies: possibilities and limitations. Int. Dairy J. 14, 273–285.
Donnelly, C.W., Briggs, E.H., Donnelly, L.S., 1987. Comparison of the heat resistance of *Listeria monocytogenes* in milk as determined by two methods. J. Food Prot. 20, 14–17.
Dos Reis-Teixeira, F.B., Alves, V.F., De Martinis, E.C.P., 2017. Growth, viability and architecture of biofilms of *Listeria monocytogenes* formed on abiotic surfaces. Braz. J. Microbiol. 48, 587–591.
Durack, J., Ross, T., Bowman, J.P., 2013. Characterisation of the transcriptomes of

genetically diverse *Listeria monocytogenes* exposed to hyperosmotic and low temperature conditions reveal global stress-adaptation mechanisms. PLoS One 8 (9), e73603.
Edelson-Mammel, S.G., Whiting, R.C., Joseph, S.W., Buchanan, R.L., 2005. Effect of prior growth conditions on the thermal inactivation of 13 strains of *Listeria monocytogenes* in two heating menstrua. J. Food Prot. 68, 168–172.
EFSA (European Food Safety Authority), ECDC (european centre for disease prevention and control), 2017. The European Union summary report on trends and sources of zoonoses, zoonotic agents and food-borne outbreaks in 2016. EFSA Journal 15 (12), 5077.
Erdogdu, F., Topcam, H., Altin, O., Verheyen, D., Van Impe, J.F., Seow, T.K., Skipnes, D., Skåra, T., 2018. Characterization of fish based model food systems for microwave heating modeling. In: Van Impe, J., Polanska, M. (Eds.), Proceedings of FOODSIM 2018. EUROSIS-ETI, pp. 235–239.
Fain Jr., A.R., Line, J.E., Moran, A.B., Martin, L.M., Lechowich, R.V., Carosella, J.M., Brown, W.L., 1991. Lethality of heat to *Listeria monocytogenes* Scott A: D-value and z-value determinations in ground beef and Turkey. J. Food Prot. 54, 756–761.
Farber, J.M., Peterkin, P.I., 1991. *Listeria monocytogenes*, a food-borne pathogen. Microbiol. Rev. 55 (3), 476–511.
Garre, A., Fernández, P.S., Lindqvist, R., Egea, J.A., 2017. Bioinactivation: software for modelling dynamic microbial inactivation. Food Res. Int. 93, 66–74.
Geeraerd, A.H., Herremans, C.H., Van Impe, J.F., 2000. Structural model requirements to describe microbial inactivation during a mild heat treatment. Int. J. Food Microbiol. 59, 185–209.
Gurtler, J.B., Marks, H.M., Jones, D.R., Bailey, R.R., Bauer, N.E., 2011. Modeling the thermal inactivation kinetics of heat resistant *Salmonella Enteritidis* and Oranienburg in 10 percent salted liquid egg yolk. J. Food Prot. 74 (6), 882–892.
Hamoud-Agha, M.M., Curet, S., Simonin, H., Boillereaux, L., 2013. Microwave inactivation of *Escherichia coli* K12 CIP 54.117 in a gel medium: experimental and numerical study. J. Food Eng. 116, 315–323.
Heertje, I., 1993. Structure and function of food products. Food Struct. 12, 343–364.
Herigstad, B., Hamilton, M., Heersink, J., 2001. How to optimize the drop plate method for enumerating bacteria. J. Microbiol. Methods 44 (2), 121–129.
Hurst, A., 1977. Bacterial injury: a review. Can. J. Microbiol. 23 (8), 935–944.
Jasson, V., Uyttendaele, M., Rajkovic, A., Debevere, J., 2007. Establishment of procedures provoking sub-lethal injury of *Listeria monocytogenes, Campylobacter jejuni* and *Escherichia coli* O157 to serve method performance testing. Int. J. Food Microbiol. 118, 241–249.
Jeanson, S., Floury, J., Gagnaire, V., Lortal, S., Thierry, A., 2015. Bacterial colonies in solid media and foods: a review on their growth and interactions with the micro-environment. Front. Microbiol. 6, 1264.
Juneja, V.K., Eblen, B.S., Marks, H.M., 2001. Modeling non-linear survival curves to calculate thermal inactivation of *Salmonella* in poultry of different fat levels. Int. J. Food Microbiol. 70, 37–51.
Khoo, K.Y., Davey, K.R., Thomas, C.J., 2003. Assessment of four model forms for predicting thermal inactivation kinetics of *Escherichia coli* in liquid as affected by combined exposure time, liquid temperature and pH. Food Bioprod. Process. 81, 129–137.
Kotrola, J.S., Conner, D.E., 1997. Heat inactivation of *Escherichia coli* O157:H7 in Turkey meat as affected by sodium chloride, sodium lactate, polyphosphate, and fat content. J. Food Prot. 60, 898–902.
Lou, Y., Yousef, A.E., 1996. Resistance of *Listeria monocytogenes* to heat after adaptation to environmental stresses. J. Food Prot. 59, 465–471.
Mackey, B.M., Kelly, A.F., Colvin, J.A., Robbins, P.T., Fryer, P.J., 2006. Predicting the thermal inactivation of bacteria in a solid matrix: simulation studies on the relative effects of microbial thermal resistance parameters and process conditions. Int. J. Food Microbiol. 107, 295–303.
Malakar, P., Brocklehurst, T.F., Mackie, A., Wilson, P., Zwietering, M., van't Riet, K., 2000. Microgradients in bacterial colonies: use of fluorescence ratio imaging, a non-invasive technique. Int. J. Food Microbiol. 56 (1), 71–80.
Mastwijk, H.C., Timmermans, R.A.H., Van Boekel, M.A.J.S., 2017. The Gauss-Eyring model: a new thermodynamic model for biochemical and microbial inactivation kinetics. Food Chem. 237, 331–341.
McMeekin, T.A., Olley, J., Ratkowsky, D.A., Ross, T., 2002. Predictive microbiology: towards the interface and beyond. Int. J. Food Microbiol. 73 (2–3), 395–407.
Meldrum, R., Brocklehurst, T.F., Wilson, D., Wilson, P., 2003. The effects of cell immobilization, pH and sucrose on the growth of *Listeria monocytogenes* Scott A at 10 °C. Food Microbiol. 20 (1), 97–103.
Miller, F.A., Brandão, T.R.S., Teixeira, P., Silva, C.L.M., 2006. Recovery of heat-injured *Listeria innocua*. Int. J. Food Microbiol. 112 (3), 261–265.
Moats, W.A., Dabbah, R., Edwards, V.M., 1971. Interpretation of nonlogarithmic survivor curves of heated bacteria. J. Food Sci. 36, 523–526.
Murphy, R.Y., Marks, B.P., Johnson, E.R., Johnson, M.G., 2000. Thermal inactivation kinetics of *Salmonella* and *Listeria* in ground chicken breast meat and liquid medium. J. Food Sci. 65 (4), 706–710.
Noriega, E., Velliou, E.G., Van Derlinden, E., Mertens, L., Van Impe, J.F., 2013. Effect of cell immobilization on heat-induced sublethal injury of *Escherichia coli, Salmonella* Typhimurium and *Listeria innocua*. Food Microbiol. 36, 355–364.
Oliveira, R.B.A., Baptista, R.C., Chincha, A.A.I.A., Conceição, D.A., Nascimento, J.S., Costa, L.E.O., Cruz, A.G., Sant'Ana, A.S., 2018. Thermal inactivation kinetics of *Paenibacillus sanguinis* 2301083PRC and *Clostridium sporogenes* JCM1416MGA in full and low fat "requeijão cremoso". Food Control 84, 395–402.
Passos, M.H.C.R., Kuaye, A.Y., 2002. Influence of the formulation, cooking time and final internal temperature of beef hamburgers on the destruction of *Listeria monocytogenes*. Food Control 13, 33–40.
Perni, S., Chalise, P.R., Shama, G., Kong, M.G., 2007. Bacterial cells exposed to nanosecond pulsed electric fields show lethal and sublethal effects. Int. J. Food Microbiol. 120 (3), 311–314.
Pin, C., Sutherland, J.P., Baranyi, J., 1999. Validating predictive models of food spoilage organisms. J. Appl. Microbiol. 87, 491–499.
Rajkovic, A., Smigic, N., Devlieghere, F., 2010. Contemporary strategies in combating microbial contamination in food chain. Int. J. Food Microbiol. 141, S29–S42.
Rawson, A., Patras, A., Tiwari, B.K., Noci, F., Koutchma, T., Brunton, N., 2011. Effect of thermal and non thermal processing technologies on the bioactive content of exotic fruits and their products: review of recent advances. Food Res. Int. 44, 1875–1887.
Reichart, O., 1994. Modelling the destruction of *Escherichia coli* on the base of reaction kinetics. Int. J. Food Microbiol. 23, 449–465.
Reiner, M., 1926. Über die Strömung einer elastichen Flüssigkeit durch eine Kapillare. Kolloid Z. 39, 80–87.
Rosnes, J.T., Skåra, T., Skipnes, D., 2011. Recent advances in minimal heat processing of fish: effects on microbiological activity and safety. Food Bioprocess Technol. 4, 833–848.
Schultze, K.K., Linton, R.H., Cousin, M.A., Luchansky, J.B., Tamplin, M.L., 2007. Effect of preinoculation growth media and fat levels on thermal inactivation of a serotype 4b strain of *Listeria monocytogenes* in frankfurter slurries. Food Microbiol. 24, 352–361.
Silva, A., Genovés, S., Martorell, P., Zanini, S.F., Rodrigo, D., Martinez, A., 2015. Sublethal injury and virulence changes in *Listeria monocytogenes* and *Listeria innocua* treated with antimicrobials carvacrol and citral. Food Microbiol. 50, 5–11.
Skandamis, P.N., Yoon, Y., Stopforth, J.D., Kendall, P.A., Sofos, J.N., 2008. Heat and acid tolerance of *Listeria monocytogenes* after exposure to single and multiple Sublethal stresses. Food Microbiol. 25, 294–303.
Skåra, T., Rosnes, J.T., Sivertsik, M., 2002. Safe and sound: minimally processed fish products. Food Technol. Int. 2, 75–76.
Skipnes, D., van der Plancken, I., Van Loey, A., Hendrickx, M., 2008. Kinetics of heat denaturation of proteins from farmed Atlantic cod (*Gadus mohua*). J. Food Eng. 85, 51–58.
Smelt, J.P.P.M., Brul, S., 2014. Thermal inactivation of microorganisms. Crit. Rev. Food Sci. Nutr. 54 (10), 1371–1385.
Suo, B., Shi, C., Shi, X., 2012. Inactivation and occurrence of sublethal injury of *Salmonella* Typhimurium under mild heat stress in broth. J. Verbr. Lebensm. 7, 125–131.
Szlachta, K., Keller, S.E., Shazer, A., Chirtel, S., 2010. Thermal resistance of *Listeria monocytogenes* Scott A in ultrafiltered milk as related to the effect of different milk components. J. Food Prot. 73 (11), 2110–2115.
Tang, S., Orsi, R.H., den Bakker, H.C., Wiedmann, M., Boor, K.J., Bergholz, T.M., 2015. Transcriptomic analysis of the adaptation of *Listeria monocytogenes* to growth on vacuum-packed cold smoked salmon. Appl. Environ. Microbiol. 81 (19), 6812–6824.
Uyttendaele, M., Rajkovic, A., Van Houteghem, N., Boon, N., Thas, O., Debevere, J., Devlieghere, F., 2008. Multi-method approach indicates no presence of sub-lethally injured *Listeria monocytogenes* cells after mild heat treatment. Int. J. Food Microbiol. 123, 262–268.
Valdramidis, V.P., Geeraerd, A.H., Gaze, J.E., Kondjoyan, A., Boyd, A.R., Shaw, H.L., Van Impe, J.F., 2006. Quantitative description of *Listeria monocytogenes* inactivation kinetics with temperature and water activity as the influencing factors; model prediction and methodological validation on dynamic data. J. Food Eng. 76, 79–88.
Van Impe, J.F., Poschet, F., Geeraerd, A.H., Vereecken, K.M., 2005. Towards a novel class of predictive microbial growth models. Int. J. Food Microbiol. 100 (1–3), 97–105.
Van Netten, P., Perales, I., van de Moosdijk, A., Curtis, G.D.W., Mossel, D.A.A., 1989. Liquid and solid selective differential media for the detection and enumeration of *L. monocytogenes* and other *Listeria* spp. Int. J. Food Microbiol. 8, 299–316.
Velliou, E.G., Noriega, E., Van Derlinden, E., Mertens, L., Boons, K., Geeraerd, A.H., Devlieghere, F., Van Impe, J.F., 2013. The effect of colony formation on the heat inactivation dynamics of *Escherichia coli* K12 and *Salmonella* typhimurium. Food Res. Int. 54 (2), 1746–1752.
Verheyen, D., Baka, M., Glorieux, S., Duquenne, B., Fraeye, I., Skåra, T., Van Impe, J.F., 2018a. Development of fish-based model systems with various microstructures. Food Res. Int. 106, 1069–1076.
Verheyen, D., Bolívar, A., Pérez-Rodríguez, F., Baka, M., Skåra, T., Van Impe, J.F., 2018b. Effect of food microstructure on growth dynamics of *Listeria monocytogenes* in fish-based model systems. Int. J. Food Microbiol. 283, 7–13.
Verheyen, D., Xu, X.M., Govaert, M., Baka, M., Skåra, T., Van Impe, J.F., 2019. Food microstructure and fat content affect growth morphology, growth kinetics, and the preferred phase for cell growth of *Listeria monocytogenes* in fish-based model systems. Appl. Environ. Microbiol. https://doi.org/10.1128/AEM.00707-19. In press.
Walker, S., Brocklehurst, T.F., Wimpenny, J., 1997. The effects of growth dynamics upon pH gradient formation within and around subsurface colonies of *Salmonella* typhimurium. J. Appl. Microbiol. 82 (5), 610–614.
Wang, X., Devlieghere, F., Geeraerd, A., Uyttendaele, M., 2017. Thermal inactivation and sublethal injury kinetics of *Salmonella enterica* and *Listeria monocytogenes* in broth versus agar surface. Int. J. Food Microbiol. 243, 70–77.
Wilson, P.D.G., Brocklehurst, T.F., Arino, S., Thuault, D., Jakobsen, M., Lange, M., Farkas, J., Wimpenny, J.W.T., Van Impe, J.F., 2002. Modelling microbial growth in structured foods: towards a unified approach. Int. J. Food Microbiol. 73, 275–289.
Wu, V.C.H., 2008. A review of microbial injury and recovery methods in food. Food Microbiol. 25, 735–744.
Wuytack, E.Y., Phuong, L.D., Aertsen, A., Reyns, K.M., Marquenie, D. De Ketelaere, B., Masschalck, B., Van Opstal, I., Diels, A.M., Michiels, C.W., 2003. Comparison of sublethal injury induced in *Salmonella enterica* serovar Typhimurium by heat and by different nonthermal treatments. J. Food Prot. 66, 31–37.
Zhao, Y., Knøchel, S., Siegumfeldt, H., 2014. *In situ* examination of *Lactobacillus brevis* after exposure to an oxidizing disinfectant. Front. Microbiol. 5, 635.